Evidence of Hydrocarbon Seepage Using Multispectral Satellite Imagery, Kurdistan, Iraq*

Sandra L. Perry[1] and Fred A. Kruse[2]

Search and Discovery Article #40694 (2011)
Posted February 15, 2011

*Adapted from expanded abstract oral presentation at AAPG International Conference and Exhibition, Calgary, Alberta, Canada, September 12-15, 2010

[1]Perry Remote Sensing LLC, Denver, CO (sandyp@rm.incc.net)
[2]Horizon GeoImaging LLC, Frisco, CO

Introduction

The petroleum system in northern Iraq has reached a maximum expulsion phase, characterized by tectonic uplift, beveled fold and thrust structures, and active surface oil seeps (Versfelt, 2001; Pitman et al., 2004). While conducting photogeologic interpretation in the region, it was observed that well exposed dip slopes exhibit spectral changes along strike, especially notable along producing antiforms near Kirkuk, Irbil, and Mosul. Proposed altered outcrops include clastic and carbonate composition, as modeled from Landsat Enhanced Thematic Mapper (ETM) and ASTER (Advanced Spaceborne Thermal Emission and Reflection Radiometer) multispectral bands. The spatial pattern of alteration does not appear to reflect lithology but is closely coincident with structure, manifested along thrusted fold fronts and eroded symmetric folds. In addition, many altered exposures correspond with known oil seeps, sour (sulfurous) water locations, and bituminous sites identified throughout the region.

Predicting and mapping rock and soil alteration from satellite imagery is an accepted practice for mineral exploration, where heat and chemical changes from intrusions alter country rocks in phases that can be spectrally characterized and associated with ore (Kruse, 1997, Kruse, et al, 2002, Perry, 2004). Geochemical alteration is noted in rocks associated with hydrocarbon microseepage and changing pH, but relatively few investigations document this approach (Schumacher, 1996, 2010). It is proposed that hydrocarbon migration has altered surface rocks in Kurdistan as evidenced by digital image analysis of Landsat and ASTER satellite imagery. Spectral measurements of hand samples collected within suspect terrain show strong indicators of alteration mineralogy from exposed upper and lower Fars Formation. While still preliminary, the mineral jarosite appears ubiquitous in hand samples tested so far suggesting acidic, sulfate-rich surface conditions not normally associated with lithology of the region.

Research is on-going and will focus on further analytical testing of both altered and unaltered exposures as well as spectral characterization and mapping using multispectral, orbiting sensors. In addition, satellite imagery proved successful for enhancing oil films on the Tigris River reservoir and in identifying active sulfurous drainage. Satellite image analysis is shown to be a key exploration tool for this geologically complex and rugged terrain.

Project Area

The area under investigation covers approximately 32,000 square kilometers of Kurdistan, an oil-rich region of northern Iraq (Figure 1). This remote location lies along the northwest-southeast trending, continent-to-continent convergent margin where the Arabian platform is colliding with and subducted by the Eurasian plate (Beydoun, 1991). Forming the rugged Zagros Mountain range, this suture zone is characterized by miogeosynclinal shelf sediments of Mesozoic and lower Paleozoic age in a fold-and-thrust structural domain (Ameen, 1991, 1992). Lateral forces have created a variety of southward-directed thrusting and northwest-southeast trending folding of the Zagros sediments, ranging from symmetric, elongated, and plunging closed folds to tightly folded, asymmetric, vertical to overturned bedding (Dunnington, 1958; Prost, 1989; Al-Gailani, 2003). The region exhibits striking anticlinal landforms expressing various stages of breaching with classic geomorphic expressions of tilted dip slopes (or cuestas), subsequent/consequent valleys, drainage patterns, and regional faulting. Pervasive northeast-trending rivers are observed cross cutting structural strike, examples of antecedent or fault-controlled drainage. Variable pulses of compression involving crystalline basement underscore the complexity of the Zagros structural belt, effecting local stratigraphy, compartmentalization, and reactivated structure throughout the suture zone and fold belt.

The climate of the region is very conducive to remote sensing evaluation, offering good exposures in a semi-arid climate with limited and clustered vegetation. Drainage features range from braided streams with alluvial fans to incised, steep canyons, and wadis. Topographic settings contrast from open rangeland to tight badlands terrain. Overall relief for the project area is calculated at approximately 3,590 meters, reflecting the intense ruggedness of the mountain range.

Imagery Data and Enhancement

Digital data for both Landsat Enhanced Thematic Mapper (ETM) and ASTER (Advanced Spaceborne Thermal Emission and Reflection Radiometer) satellite imagery were obtained to cover the project area. Scenes were mosaicked and orthorectified to UTM Zone 38N, WGS'84 map base. Landsat visible and near-IR (VNIR) bands 1, 2, and 3 were combined with ASTER short-wave IR (SWIR) bands 5, 6, 7, 8, and 9 to create a hybrid and optimum data set for image analysis. All bands were co-registered at 30-meter spatial resolution (or pixel size). In addition, Landsat and ASTER spectral bands require atmospheric correction.

In order to enhance altered exposures and generic rock and soil composition, prepared image masks suppress unwanted vegetation, dark-target (i.e., shadows), snow, and water spectral responses. Typically, Landsat and ASTER reflectance bands show a high degree of statistical correlation. Therefore once spectral bands are adequately masked, VNIR and SWIR bands are transformed using ratioing and principle-component techniques, thereby accentuating spectral characteristics that aid in predicting composition as well as altered rock and soil exposures. An example of Landsat decorrelated reflectance bands for Baba Dome oil field is shown in Figure 2.

Altered exposures demonstrate a strong correlation with known oil producing fields, breached antiforms, and mapped oil seep/sour water/bituminous sites. Predicting the mineralogy of these spatial coincidences is significant to exploration and understanding alteration systems associated with hydrocarbons. The Zagros Mountains example offers an excellent case history for remote sensing, because of documented oil production and seepage as well as exposures of beveled, altered anticlines, where hydrocarbons have already been expelled. Altered locations near Pulkhana, Kor Mor, and Kirkuk oil fields identified training sites for supervised classification (on decorrelated, masked input bands) throughout the entire project area offering good results, coincident with other oil seep and sour water/bituminous sites. Therefore, the next phase of image analysis would seek to identify minerals associated with altered exposures near production and seeps.

Prepared and masked Landsat/ASTER data were then evaluated using image classification algorithms (Spectral Feature Fitting, or SFF, and Spectral Angle Mapper, or SAM offered in ENVI Image Processing Software) with public-domain spectral mineral libraries (USGS: Clarke et al, 2007; John Hopkins Spectral Library: Salisbury et al, 1991). Spectral libraries are resampled to fit the hybrid Landsat/ASTER wavelength intervals, and an image analysis tool compares image spectra for pixels in suspected altered locations to known mineral spectra in spectral libraries, listing alteration mineralogy matches. This approach is known as mineral modeling and is utilized when no ground truth information is available. Several mineral models were predicted and mapped: fine- grained calcite, dolomite, chlorite/epidote, illite, smectite, gypsum, Mg-Al/Ca-Mg silicates, and FeOx.

Ground-truth Samples

To test mineral models, hand samples are collected for direct spectral measurements and mineral identification within suspected altered areas. Fortunately, field personnel were available for this task but only for certain regions of the project area, limited due to safety and access. Rock samples collected within proposed altered locations were documented with GPS positions and shipped to Denver for analysis employing an ASD field-portable spectrometer (Analytical Spectral Devices, Inc., Boulder, Colorado USA). Spectral mineral id work indicated various mineral mixtures for calcite, illite, jarosite, and Fe. The surprising alteration mineral occurrence of jarosite is significant since this iron-sulfate mineral is an indicator of acidic, sulfate-rich conditions (Swayze et al., 2008). The majority of 30 hand samples exhibited jarosite composition even in combination with calcite, which is not typical.

In reviewing hand sample mineral identification with mineral models, it appears that calcite and illite have been confirmed. Revisiting the GPS coordinates on the imagery show that for these locations, Landsat/ASTER mineral models were successful for predicting mineral composition. No hand samples were collected for sites with proposed dolomite, chlorite/epidote, gypsum, or Mg-Al/Ca-Mg silicates, so these remain unconfirmed. Closer inspection reveals that smectite and FeOx, modeled from Landsat/ASTER hybrid imagery, may actually reflect jarosite occurrence. Multispectral wavelengths are likely too coarse to uniquely resolve jarosite using the mineral spectra- matching classification approach. However, since jarosite has been verified in hand samples with known locations, training sites were outlined and offered successful supervised classification performed on the masked, decorrelated band set.

Discussion and Conclusions

Hand samples for this investigation were collected along the eastern extension of Kor Mor oil field within exposures of upper and lower Fars Formation, a lagoonal interbedded sequence of sandstone, shale, anhydrite, and limestone units of middle Miocene age (Konert et al., 2001). Calcite has been found in nearly half of the hand samples and may reflect original limestone composition. Or, calcite may be an alteration product of hydrocarbon seepage, altering gypsum to carbonate (Donovan, 1974). Illite may be an in-situ mineral associated with clastic facies but could also reflect altered phases of silty and sandy interbedded units.

Jarosite is commonly found in acidic soils associated with mine waste formed by the oxidation of sulfide minerals (Swayze et al., 2008). Jarosite found in this environment may reflect highly acidic conditions associated with sulfurous hydrocarbon seepage. Other investigators have identified jarosite with subsurface hydrocarbon reservoirs (Buckingham and Sommer, 1983; Everett et al., 2002), so finding it at the surface in a seep-prone environment may not be unexpected. In the project area, field observations have confirmed sulfurous water sites including one such location where stream pH was so altered, water-color was changed due to higher dissolved minerals (W. Matthews, personal communication). This water-color change was enhanced, characterized, and mapped using high-spatial resolution (hi-res) QuickBird (QB) true color imagery. In addition, oil films were enhanced and mapped using multispectral imagery on the Tigris River reservoir, located in the northern portion of the project area. Oil films are spatially coincident with fields mapped on either side of the reservoir that are leaking into the lake.

While other multispectral mineral models will require additional field testing, spectrally characterizing jarosite throughout the region has demonstrated spatial coincidence with other known oil production and seepage and, therefore, appears to be a significant mineral to predict and map.

References

Al-Gailani, M., 2003, Assessing Iraq's oil potential: Geotimes, October 2003. https://www.agiweb.org/geotimes/oct03/feature_oil.html

Ameen, M. S., 1992, Effects of basement tectonics on hydrocarbon generation, migration, and accumulations in northern Iraq: AAPG Bulletin: v. 76, p. 356-370.

Ameen, M. S., 1991, The significance of strike-slip faulting in the basement of the Zagros Fold and Thrust Belt: Journal of Petroleum Geology: v. 24, p. 5-28.

Beydoun, Z. R., 1991, Arabian Plate Hydrocarbon Geology and Potential, a Plate Tectonic Approach: AAPG Studies in Geology 33, 70 p.

Buckingham, W.F. and S.E. Sommer, 1983, Mineralogical characterization of rock surfaces formed by hydrothermal alteration and weathering – application to remote sensing: Economic Geology, v. 78, p. 664-674.

Clark, R.N., G.A. Swayze, R. Wise, E. Livo, T. Hoefen, R. Kokaly, and S.J. Sutley, 2007, USGS digital spectral library splib06a: U.S. Geological Survey, Digital Data Series 231,
http://speclab.cr.usgs.gov/spectral-lib.html

Donovan, T. J., 1974, Petroleum microseepage at Cement Oklahoma: Evidence and mechanism: AAPG Bulletin, v. 58:3, p. 429–446.

Dunnington, H.V., 1958, Generation, migration, accumulation, and dissipation of oil in northern Iraq: *in* G.L. Weeks, (ed), Habitat of Oil: AAPG Bulletin, p. 1194-1252.

Everett, J.R., R.J. Staskowski, and C. Jengo, 2002, Remote sensing and GIS enable future exploration success: World Oil, v.223:11, p. 59-60, 63-5.

Konert, G., A.M. Afifi, S.A. Al-Hajri, K. deGroot, A.A. Al Naim, and H.J. Droste, 2001, Paleozoic stratigraphy and hydrocarbon habitat of the Arabian Plate: *in* Petroleum Provinces of the Twenty First Century: AAPG Memoir 74, p. 483-515.

Kruse, F.A., 1997, Visible/infrared sensors and case histories, in Remote Sensing for the Earth Sciences, ed. A.E. Rencz, John Wiley, New York, p. 567-611.

Kruse, F.A., S.L. Perry, and A. Cabellero, 2002, Integrated multispectral and hyperspectral mineral mapping, Los Menucos, Rio Negro, Argentina, EO-1 Hyperion/AVIRIS comparisons and Landsat TM/ASTER extensions, Proceedings f 11th Airborne Geoscience Workshop: JPL Publication 03-4, p 185–188.

Perry, S.L., 2004, Spaceborne and airborne remote sensing for mineral exploration – case histories using infrared (IR) spectroscopy, *in* Infrared Spectroscopy in Geochemistry, Exploration, and Remote Sensing: Mineralogical Association of Canada, Short Course Series Volume 10; eds. P.L. King, M.S. Ramsey, and G.A. Swayze, Chapter 10, p. 227 – 240.

Pitman, J.K., D. Steinhouser, and M.D. Lewan, 2004, Petroleum generation and migration in the Mesopotamian Basin and Zagros Fold Belt of Iraq: results from basin-modeling study: GeoArabia, vol. 9, No. 4.

Prost, G. L., 1989, Recognizing thrust faults and exploration implications, *in* ERIM Proceedings of the Seventh Thematic Conference on Remote Sensing for Exploration Geology, Calgary, Alberta, Canada, Oct 2–6, 1989, p. 1111-1123.

Salisbury, J. W., L.S. Walter, N. Vergo, and D.M. D'Aria, 1991, Infrared (2.1- 25 micrometers) Spectra of Minerals, Johns Hopkins University Press, 294 p. http://speclib.jpl.nasa.gov/documents/jhu_desc

Schumacker, D., 2010, Integrating hydrocarbon microseepage data with seismic data doubles exploration success. *in* Proceedings, Indonesian Petroleum Association, 34th Annual Conference, May 2010, 14 p.

Schumacker, D., 1996, Hydrocarbon-induced alteration of soils and sediments, *in* D. Schumacker and M.A. Abrams, eds., Hydrocarbon migration and its near-surface expression: AAPG Memoir 66, p. 71-89.

Swayze, G. A., G.A. Desborough, K.S. Smith, H.A. Lowers, J.M. Hammarstrom, S.F. Diehl, R.W. Leinz, and R.L. Driscoll, 2008, Understanding jarosite – from mine waste to Mars: U.S. Geological Survey, Circular 1328, Chapter B, 13 p.

Versfelt, P.L. Jr., 2001, Major hydrocarbon potential in Iran, *in* Petroleum Provinces of the Twenty First Century: AAPG Memoir 74, p. 417-427.

Yang, H., J. Zhang, F. van der Meer, and S.B. Kroonenberg, 1998, Geochemistry and field spectrometry for detecting hydrocarbon microseepage: Terra Nova, v. 10, p. 231–235.

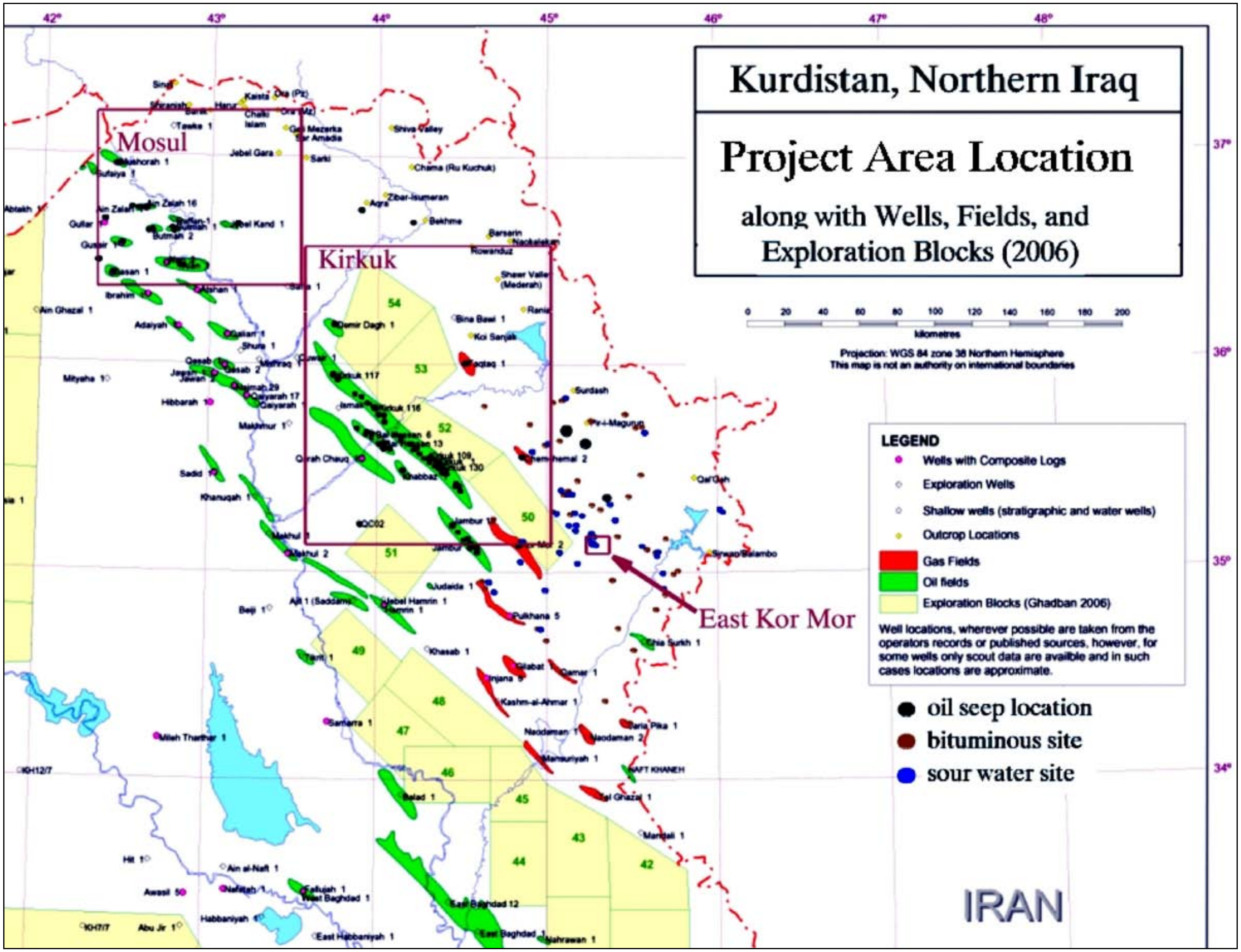

Figure 1. Project location highlights three areas in the oil-rich region of northern Iraq (dark red outlines above for Mosul, Kirkuk, and East Kor Mor). The area mapped covers approximately 32,000 square kilometers.

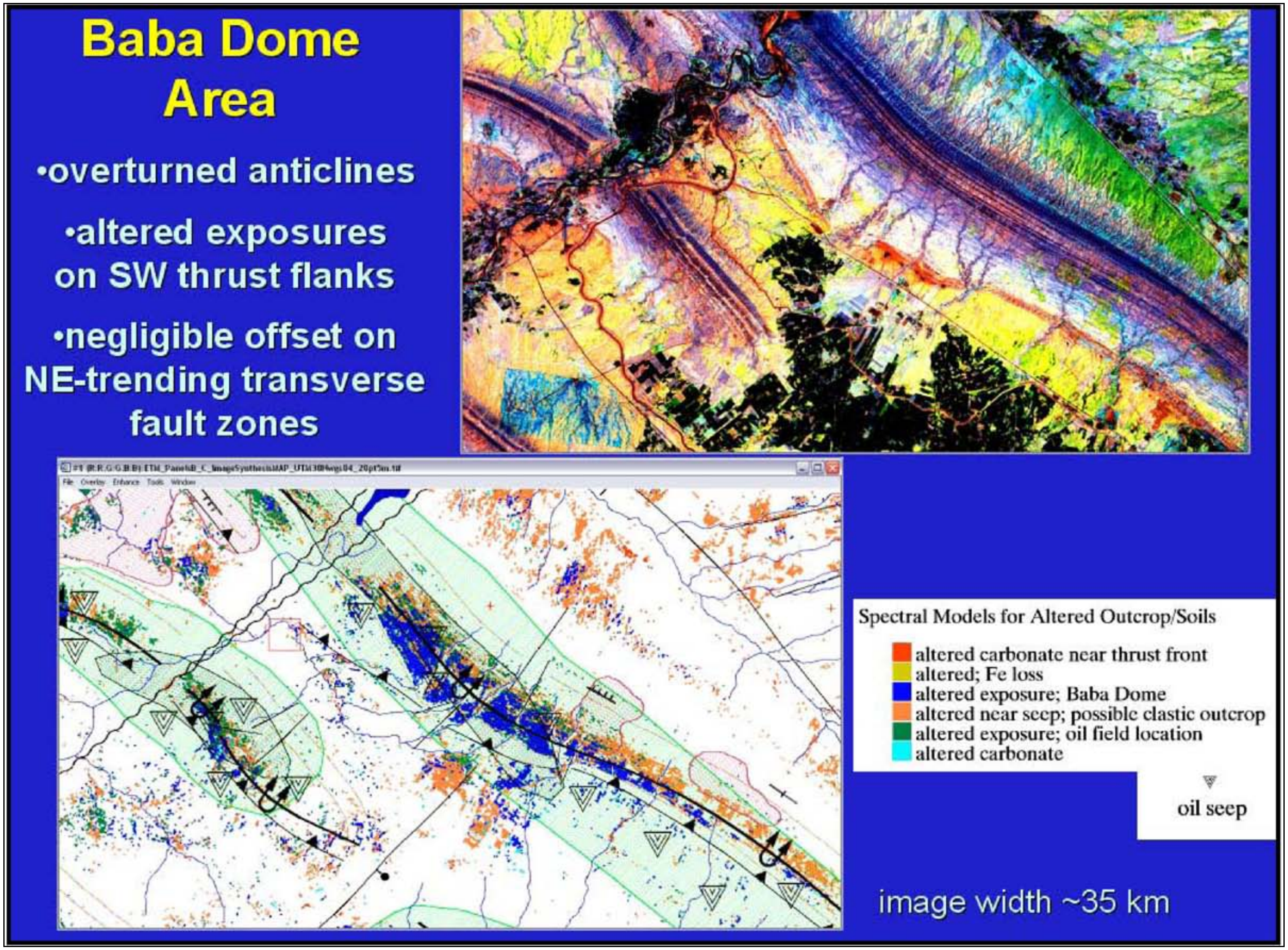

Figure 2. Enhanced Landsat image of the Baba Dome portion of the Kirkuk oil field predicting altered exposures in pastel to white colors (above right). Resulting structural interpretation shows producing oil fields in pale green polygons and proposed alteration mineral models (lower left).